Mimosa-Inspired Design of a Flexible Pressure Sensor with Touch Sensitivity

Bin Su, Shu Gong, Zheng Ma, Lim Wei Yap, and Wenlong Cheng**

Substantial recent research interest has been directed to emerging unconventional flexible/stretchable electronics. Devices of particular interest are flexible pressure sensors which have broad technological implications for areas ranging from wearable electronics,[1] real-time health monitoring[2–4] to soft robots and prosthetic devices.[5,6] Among various flexible pressure sensors developed recently,[7–13] resistance-type ones are facile to produce at large-scale and in a cost-effective manner due to their relatively simple structures and fabrication process.[14] Typically, flexible pressure sensors can be constructed by embedding conducting fillers into soft elastomeric materials forming 3D percolating networks.[15–18]

In order to further increase the sensitivity and reduce the device responding time, introducing microstructures upon 2D polymeric surfaces is critical in the device design. Pyramid,[19] micropillar,[20] interlocking[21] and aligned[22] nanofibers, and microgroove[23] shaped microstructures have been fabricated to endow the elastic materials with greatly enhanced tactile sensitivity (i.e. an increase by ≈50 times[19]). Despite significant device sensitivity has been achieved, the fabrication of above-mentioned surface microstructures largely depends on the traditional lithography technique (i.e. by molding from laser-etched silicon patterns), which is a time-consuming, high-cost process with limited scalability.

Herein, we report on a new bio-inspired strategy to fabricate flexible pressure sensors with touch sensitivity. Inspired by mimosa, a plant that can close their leaves under external stimuli, we demonstrate a simple, efficient, low-cost and scalable direct-molding method to flexible pressure sensors which are sensitive enough to mimic mimosa leaves. In the regime of 0–70 Pa, a sensitivity of 50.17 kPa^{-1} was obtained, which is higher than that for many reported flexible pressure sensors.[19–22] Our bio-inspired sensor could respond to pressure changes within 20 ms, simultaneously with negligible loading-unloading signal changes over 10 000 cycles. Furthermore, an artificial touch-sensing "mimosa leaves" has been demonstrated based on the study of touch-sensitive flexible pressure sensor. We believe that our mimosa-inspired approach opens a new route to fabricate flexible pressure sensors in a cost-effective and scalable manner.

After undergoing billions of years of evolution and natural selection, nature has gained the wisdom on how to get maximal functions at the cost of minimum resources.[24,25] Microstructures widely exist upon the surfaces of natural creatures.[26] Thanks to these unique surface constructions, animals or plants can self-repel the water permeation,[27] obtain highly dry adhesion,[28] and exhibit stimuli-responsive behaviors. *Mimosa*, a plant can close their leaves under external stimuli, is a natural example of flexible pressure sensors. Their leaves are bipinnately compound with one pair of pinnae that consists of ≈15 leaflets (**Figure 1**a). From the scanning electronic microscopy (SEM) observation of a usual leaflet, an irregular pattern of microdomains with an average diameter of 18.4 ± 6.1 μm and height of 16.1 ± 3.7 μm can be found upon the leaflet (Figure 1b–d). Owing to the existence of these protuberant microdomains, a gentle finger touching could be transferred into a biologically electric signal, leading to the release of water from the leaf cell vacuoles.[29] Then, thousands of plant cells would collapse. As a result, the leaflets will close within nearly three seconds (Supporting Information, Movie S1). Inspired from these "natural tactile sensors", we demonstrate a new strategy to fabricate flexible pressure sensors in a simple yet efficient matter.

To mimic the stimuli-responsive performance of mimosa leaves, a square piece of pre-cleaned mimosa leaflet (4×1 cm^2) was used as the template for fabricating micropatterned polydimethylsiloxane (PDMS) thin film, as illustrated in **Figure 2**a. PDMS was chosen as the device substrate in this study due to its good elastic properties, its biomedical compliance with human tissue, and its high performance as a dielectric material in flexible electronics.[30] After two-step negative/positive molding from the mimosa leaflet, PDMS films can be endowed with rough microstructures upon their surfaces. The thickness of the PDMS thin film was controlled in the range of 300 ± 40 μm. The morphology and microstructure of structured PDMS film were observed by SEM with different view angles (Figure 2c,d), which show similar microdomain patterns to that of the mimosa leaflet (Figure 1b,c).

After generating rough and flexible PDMS substrates, a thin layer of conducting gold has been deposited upon the surfaces to effectively transport the electrons. The adhesion between the electricity active layers and the flexible substrates plays an important role in deciding the lifetime of pressure sensors. Several groups reported the appearance

Dr. B. Su, S. Gong, Z. Ma, L. W. Yap, Prof. W. Cheng
Department of Chemical Engineering
Monash University
Clayton, Victoria 3800, Australia
E-mail: bin.su@monash.edu;
wenlong.cheng@monash.edu
Prof. W. Cheng
The Melbourne Centre for Nanofabrication
Clayton, Victoria 3800, Australia

DOI: 10.1002/smll.201403036

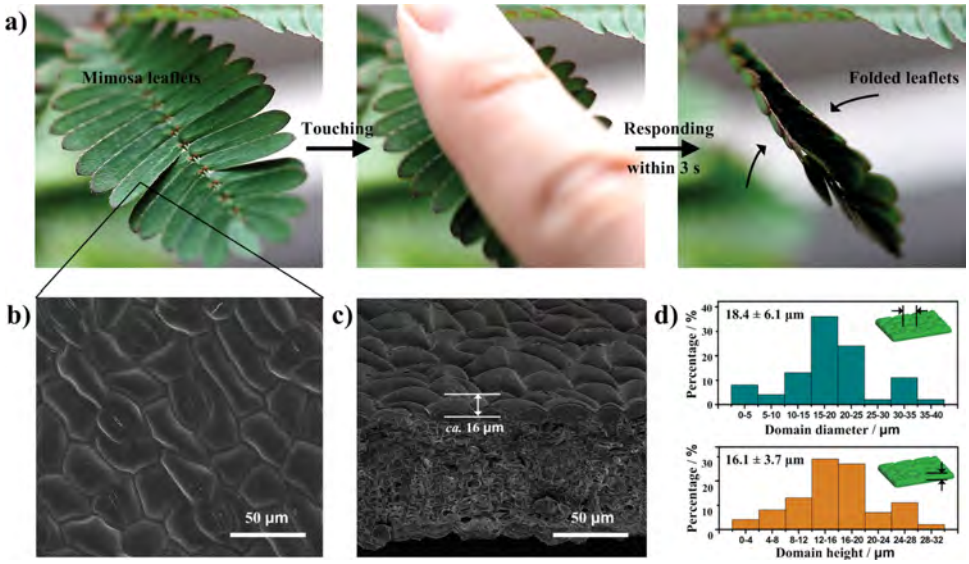

Figure 1. "Naturally" flexible pressure sensors of *mimosa* leaves. a) Digital photographs of mimosa leaves. They are a bipinnately compound with one pair of pinnae that consists of ≈15 leaflets. A gentle touch by one human finger can yield the leaflets closing within less than three seconds. b) Top and c) side view scanning electronic microscopy (SEM) observations of a usual leaflet, showing the existence of an irregular microdomain pattern. The height of microdomains is ca. 16 μm. d) Statistical histograms of the microdomain diameter (top) and height (bottom) obtained from 50 regions.

of cracks of rigid conducting layers upon PDMS surfaces after thousands of external stimulti,[31,32] which greatly prevents the performance of as-prepared device. To reduce the appearance of cracks, a ≈5 nm thick titanium layer has been pre-deposited to serve as the connect layer between the PDMS surface and the gold layer. Then, ≈30 nm thick gold has been anchored upon the titanium layers, resulting a resistance of 110 ± 14 Ω sq^{-1}. Owing to the existence of

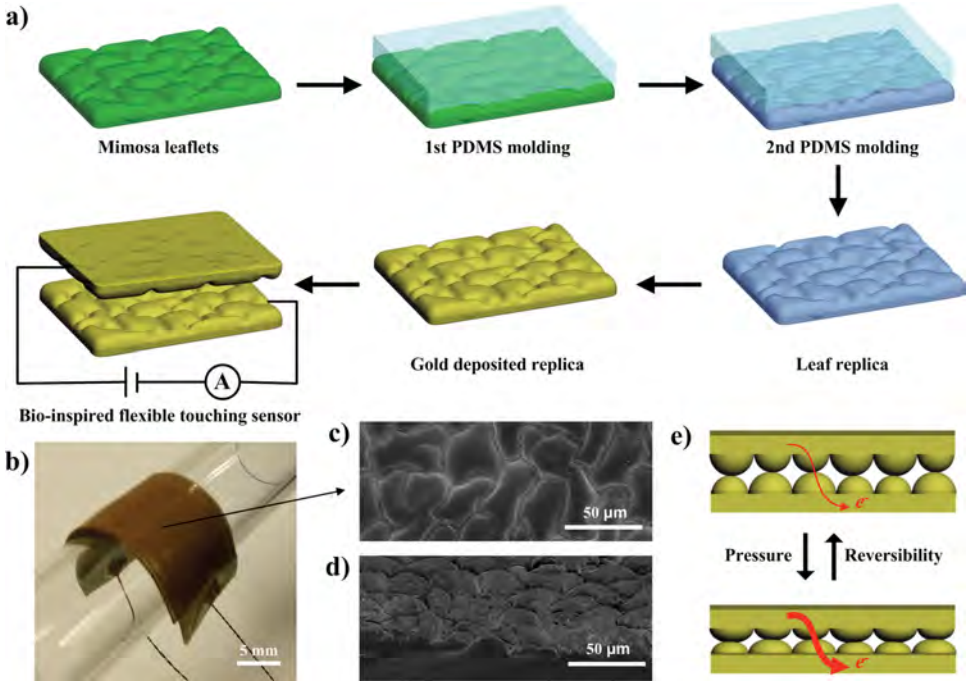

Figure 2. Polymer-based flexible pressure sensors learned from the *mimosa* leaves. a) Schematic illustration of the fabrication process of flexible microstructured PDMS films and corresponding pressure sensors. After two-step negative/positive molding from the mimosa leaflet, PDMS films can be endowed with precise surface microstructures as the plant owns. Then, a thin layer of electricity active coating has been deposited upon the microstructure to effectively transport the electrons. Finally, two layers of coated PDMS films with the microstructured surfaces have been placed as a interlocked geometry, yielding a bio-inspired pressure sensor. b) Digital photograph showing the bending ability of the sensor. c) Top and d) side view SEM observations of a molded PDMS film with the similar microstructure to that of mimosa leaves. e) Current changes in responses to pressure and reversibility. The compressive deformation of microstructure could yield the current increase and this change would return to the primary state when removing the external force.

small 2014,
DOI: 10.1002/smll.201403036

small

pre-deposited titanium layer, only few/discontinuous cracks can be found in the microdomain gaps of a sample after undergoing 10 000 pressure cycles (see the SEM observations of deposited PDMS surfaces in the Supporting Information, Figure S1). The thickness of deposited gold layer has been investigated (Supporting Information, Figure S2). Thinner ones (<20 nm) yield high resistance as well as low responsive impedance. When the thickness is more than 30 nm, stable resistance and impedance change appeared. Therefore, we chose ≈30 nm thick gold layer in this study.

Consequently, two layers of coated PDMS films with the microstructured surfaces have been placed face-to-face into an interlocked construction, and conductive wires were anchored on the edge of both films as the source-drain electrodes (Figure 2b and device details can be found in the Supporting Information, Figure S3). Therefore, a mimosa-inspired flexible pressure sensor has been fabricated. Interlocked geometry has been employed by several groups.[21,33–35] This special construction can induce external pressure concentrating at the small contact spots as well as local deformations in the microdomains. As a result, significant impedance change would appear even at a small pressure stimulti. We compared the electricity-responsive behaviors of rough-to-rough interlocked type, rough-to-flat type and flat-to-flat type devices (Supporting Information, Figure S4). Under 156 Pa applied pressure, rough-to-rough type device has generated more than 0.6 mA current increase while the flat-to-flat counterpart showed a tiny current change (≈0) and rough-to-flat one exhibited smaller change (≈0.4 mA). Therefore, rough-to-rough interlocked geometry has been used in this study.

The sensing mechanism of the device is attributed to pressing-force-dependent contact between top and bottom rough surfaces. Unlike flat thin films, a small compressive deformation of microstructured PDMS surfaces would happen when applied an external pressure, yielding increased conductive pathways and corresponding current enhancement (Figure 2e). On unloading, these microstructured PDMS films would recover to their original shapes, leading to the decrease of the current to the primary value.

The pressure sensitivity (S) of the bio-inspired polymer sensor has been tested by utilizing a computer-controlled stepping motor and a force sensor, shown in **Figure 3**a. The sensitivity S can be defined as:

$$S = \frac{\frac{I - I_{off}}{I_{off}}}{\Delta P} \quad (1)$$

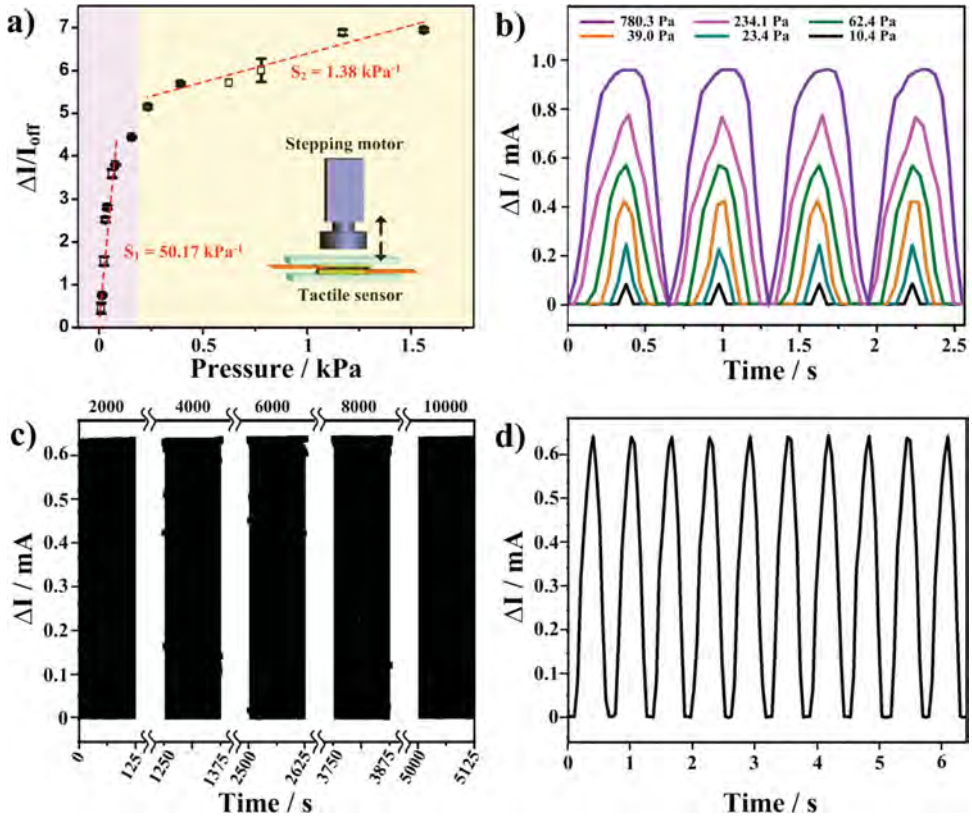

Figure 3. High-sensitivity, stable and reliable flexible pressure sensors. a) Pressure-response plots for the bio-inspired pressure sensor. The structured PDMS films exhibit a high pressure sensitivity of 50.17 kPa^{-1} during 0 and 70 Pa and relatively low pressure sensitivity of 1.38 kPa^{-1} during 200 and 1500 Pa. The inset image is schematic of the experimental set-up. A force sensor and a stepping motor connected with a computer were utilized to control the applied pressure and frequency. b) Plots of current response of the sensor as a function of time (pressure input frequency: 1.6 Hz) for the applied pressures in the range of 10.4 – 780.3 Pa. c) The life-time test under a pressure of 156 Pa at a frequency at 1.6 Hz. The current change curves were recorded after each 2000 cycles and 200 cycles of data were presented in each recording. d) Magnified view of the part of the ΔI–t curve in c) after 10 000 loading–unloading cycles. The applied voltage is 10 mV in all tests.

DOI: 10.1002/smll.201403036

Where I is the current when applied pressure on the devices, and I_{off} is the current of device with only base pressure; ΔP is the change of applied pressure.

The points in Figure 3a can be divided into two regions based on difference in sensitivity. In the low pressure region (purple region, 0–70 Pa), the sensitivity of the device is 50.17 kPa^{-1}, which is much higher than that of the relatively large pressure region (1.38 kPa^{-1} in yellow region, 200–1500 Pa). The separated fittings of these points in both regions showed good linear behaviors (R_{purple}^2 = 0.943, and R_{yellow}^2 = 0.961, see Supporting Information, Figure S5a,b), indicating the device can serve as a reliable pressure sensor. The reason for different sensitivities can be explained on the basis of the previous reports.[19–23] In low-applied-force purple region, the pressure increase resulted in decreased gap between top/bottom microdomains, yielding close contact between the microstructures. In contract, it is quite possible that the gap distance has already reached zero from the turning point in yellow region, and further increasing pressure only works for enhancing the microdomain deformation. In other words, the contact area tended to saturate in yellow region, and the applied pressure has little effect on the current variation. This trend became more obvious in larger pressure ranged from 2 kPa to 10 kPa (see Supporting Information, Figure S5c). Briefly, high device sensitivity of 50.17 kPa^{-1} (0–70 Pa) can be generated by this bio-inspired pressure sensor, which is larger than most reported records in flexible pressure sensors.[19–22] So far as we know, only Bao's group reported a higher sensitivity value ≈56.0–133.1 kPa^{-1} with pressure range from 0 to 30 Pa.[23] The significant change in resistance of the interlocked microdomain arrays could be contributed by the deformation of microdomain structures and the resulting variation in contact area.

The responses of our bio-inspired sensors to both static and dynamic mechanical pressures were characterized. The sensor exhibited a steady response to static pressure and the resistance under each pressure applied (Supporting Information, Figure S6). The resistance became saturated when the applied pressure > ~1 kPa, this result fits the sensitivity measurement well. To investigate the pressure range of our bio-inspired sensors towards dynamic forces, a piezoelectric stepping positioner with minimum displacement of only 1 mm was applied to the sensors. As shown in Figure 3b, a pressure of 10.4 Pa could be detected, which indicates the weight of a water droplet (~10.4 μl) on a surface of 10 mm^2. At the higher pressure range (0.5–1 kPa), the noise-free, stable continuous responses could be observed. The width of responding peaks is not uniform due to the mechanical parameter of force detector (see experimental section). The cycling stability of our prepared bio-inspired pressure sensor was tested under a pressure of 156 Pa at a frequency of 1.6 Hz (Figure 3c,d). The consistent resistance change with pressure applied on the surface of the pressure sensor can be maintained after 10 000 loading–unloading cycles, implying long working life and reliability of this bio-inspired pressure sensor.

To investigate the response time of our sensors to applied forces, the output current signals and the dynamic pressure inputs have been compared, showing a ≈20 ms response hysteresis (Supporting Information, Figure S7). In addition to pressing forces, this bio-inspired pressure sensor could simultaneously be utilized to detect the bending force (Supporting Information, Figure S8). This device exhibited stable responses to various bending angles by employing a stepping machine. The responsive impedance remains stable even after 5000 bending cycles, indicating the reliability of this device.

We further used our bio-inspired pressure sensors to build an "artificial mimosa leaves" with an integrated system of "touching-responding-feedback", shown in **Figure 4**a. Three pairs of "bio-inspired pressure sensors" have been cut into natural leaflet shapes, and placed onto a 3D-printed bracing frame (Figure 4b). These flexible pressure sensors were connected with two control parts: the electrical part served as the function of "touching-responding" while the mechanical system worked for the behavior of "responding-feedback". Furthermore, we tailored the lengths of physically connecting lines to mimic different closing levels of the leaflets. Once a pressure-sensor leaflet has been touched (Figure 4c), the external force could be transferred into a changed electrical signal, and triggered the motor to rotate. This process is similar to the performance of natural mimosa leaves. Owing to the unidirectional rotating of the motor, the lines connected with the leaflet pairs would be tightened up, yielding the closing of "artificial mimosa leaflets" (Figure 4d). This mechanism is to repeat the cell-collapse-induced closing of natural leaves by utilizing a simple mechanical process. Finally, the whole performance of this "artificial mimosa leaves" has been fulfilled within one second (Supporting Information, Movie S2), which is quicker than the natural counterpart (Figure 1).

Besides *mimosa*, the leaves of other plants, such as *cymbopogon citratus* or *populus lasiocarpa*, have also been employed to generate flexible pressure sensors in similar processes (Supporting Information, Figure S9). The optimal height for piezoresistive pressure sensors can range form several hundreds of nanometers[21] to nearly half a micrometer[23]. Unfortunately, the height of microstructures upon *cymbopogon citratus* in this study was too large (≈78 μm) to deposit continuous electricity active coating, leading to the block of electron transport. *Cymbopogon citratus*, on the other hand, owned smaller microstructure height and enabled successful generation of pressure sensor. However, the current change was smaller than that of *mimosa* at the same applied pressure. In this control experiment, it is obvious that the height of surface microstructures played an important role in deciding the sensor sensitivity. Carefully choosing the plant template type, such as the *mimosa*, would yield great performance of bio-inspired pressure sensors.

In summary, we demonstrate that naturally microstructured plant leaves can serve as low-cost and environment-friendly templates for fabricating super-sensitive, rapid-responding and reliable pressure sensors at low cost. These bio-inspired contact-resistance-type pressure sensors show advantages such as high sensitivity (50.17 kPa^{-1}), quick responding time (<20 ms), and durable stability (negligible loading-unloading signal changes over 10 000 cycles). Importantly, the whole device fabrication process is facile without the need of complex or expensive equipment. We believe that our methodology opens a new route to low-cost flexible pressure sensors with a wide range of applications in future wearable electronics.

small 2014,
DOI: 10.1002/smll.201403036

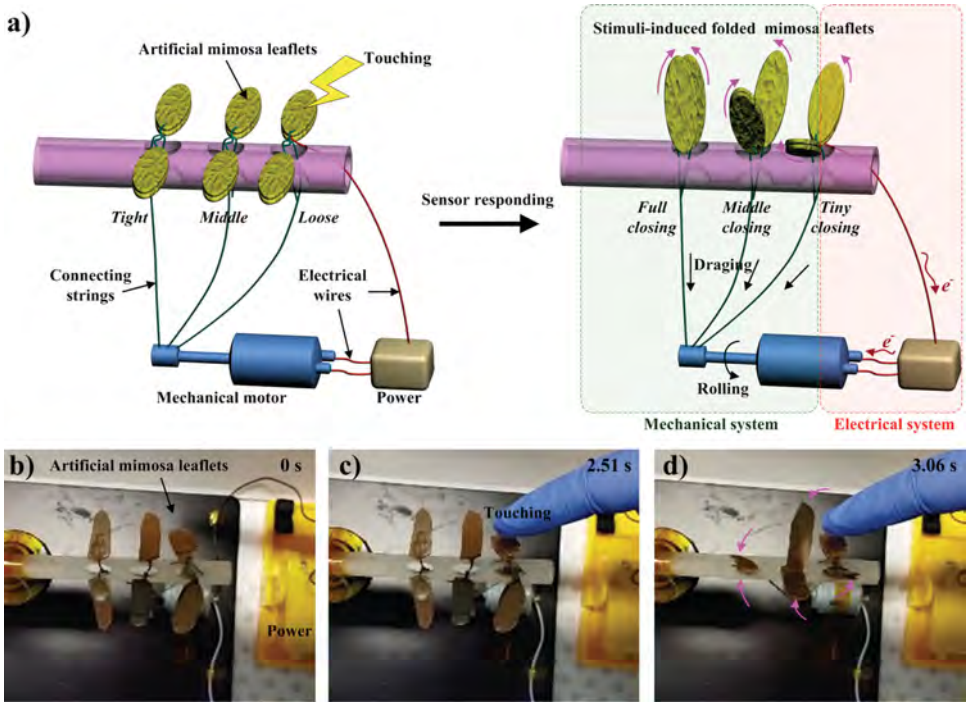

Figure 4. An "artificial mimosa leaves" with an integrated system of "touching-responding-feedback". a) Schematic illustration of the generation of "artificial mimosa leaves". A rigid polymeric bracing frame with three holes has been generated by the 3D-printer. Then, bio-inspired flexible pressure sensors have been cut into natural leaflet shapes and placed onto the bracing frame. These flexible pressure sensors were connected with two control parts: the electrical part served as the function of "touching-responding" while the mechanical system worked for the behavior of "responding-feedback". The lengths of physically connecting line have been tailored to mimic different closing levels of the leaflets. b–d) Digital photographs of the performance of "artificial mimosa leaves". Once a pressure-sensor leaflet has been touched, the external force could be transferred by the sensor into a changed electrical signal, and triggered the motor to rotate. Owing to the unidirectional rotating of the motor, the lines connected with the leaflet pairs would be tightened up, yielding the closing of "artificial mimosa leaflets" within one second. The voltage of power is 3 V (two A5 batteries).

Experimental Section

Preparation of Flexible Microstructured PDMS Conducting Films: First, the leaves of plants, such as *mimosa*, *cymbopogon citratus* or *populus lasiocarpa*, have been cut into 4×1 cm^{-2} (might need several leaves due to their limited surface areas) and washed with deionized water for 10 min, followed by sonication in deionized water for 20 min. Then, they were blown dry with a nitrogen gun to get pieces of pre-cleaned plant templates. Secondly, the fabrication of microstructured PDMS film is performed. Polydimethylsiloxane (Sylgard 184) precursor was mixed with a curing agent in the proportion of 10:1 by weight. The PDMS mixture was put into a centrifuge to remove air bubbles (2000 rpm, 5 min). Then the mixture was poured onto the plant templates. To make great replicating of the leave surfaces, the remaining air bubbles between the PDMS and leaves were removed in a vacuum chamber. After heating at 60 °C for 4 h, the leaves were carefully peeled. Then, a PDMS negative template was modified using fluoride molecules (heptadecafluorodecyltrimethoxysilane) in a decompressed environment at room temperature for 24 h and then heated at 80 °C for 3 h. The fluoride molecules could decrease the surface energy of PDMS negative templates and facilitate the peeling of positive microstructures. To fabricate softer PDMS positive replica, toluene-diluted PDMS (PDMS:toluene = 5:1 w/w) was poured on the modified negative template and then cured at 80 °C for 3 h. The artificial PDMS leaves with similar plant surface microstructures were also carefully peeled off the negative template. Thirdly, to introduce a thin layer of electricity active coating onto the PDMS microstructures, Ti/Au interdigitated coating (Thickness at 5 nm/30 nm) were gradually deposited using an electric beam evaporator (Intlvac Nanochrome II, 10 kV). Finally, two layers of coated PDMS films with the microstructured surfaces have been placed face-to-face, and conductive wires was anchored on the edge of both films as the source-drain electrodes, yielding the generation of bio-inspired flexible pressure sensors.

Fabrication of "Artificial Mimosa Leaves": A rigid polymeric bracing frame with three holes has been generated by the 3D-printer (Objet Eden 260V). Then, bio-inspired flexible pressure sensors have been cut into natural leaflet shapes and placed onto the bracing frame. These flexible pressure sensors were connected with two control parts: the electrical part served as the function of "touching-responding" while the mechanical system worked for the behavior of "responding-feedback". The motor for receiving the electrical signal and giving mechanical feedback was detached from a fan toy purchased from ebay online.

Characterization: SEM images were characterized using a FEI NovaNanoSEM 430 operated at 5 kV beam voltage. The sheet resistances of coated PDMS substrates were carried out on a Jandel four point conductivity probe by using a linear arrayed four point head. The current differences and the I-V characteristics for the pressure sensor were recorded by the Parstat 2273 electrochemical system (Princeton Applied Research). For the dynamic

DOI: 10.1002/smll.201403036

low pressure measurement, a piezoelectric stepping positioner (SLC-1730) was used by a custom LabView programme and the force data was measured by an electrical balance (Mettler Toledo NewClassic MF, MS105DU). The value of applied pressure can be adjusted by increasing the distance between the pressure step and the sample. Therefore, the contacting time between the pressure step and the sample is different, yielding various widths of responding peaks. For the bending investigation, the sensor has been fixed and bent by a stretchable machine (Thorlebs, LTS150/M).

Supporting Information

Supporting Information is available from the Wiley Online Library or from the author.

Acknowledgements

This research was financially supported under the Australian Research Council's Discovery Early Career Researcher Award (DECRA) funding scheme (DE140100541) and Discovery projects funding scheme (DP120100170 and DP140100052). The authors also acknowledge Romiza Mazid (Monash University, Australia) and Xiaonan Kan (Institute of Chemistry, Chinese Academy of Science, China) for helpful experimental assistances. This work was performed at the Melbourne Centre for Nanofabrication (MCN) in the Victorian Node of the Australian National Fabrication Facility (ANFF).

[1] a) M. L. Hammock, A. Chortos, B. C. Tee, J. B. Tok, Z. Bao, *Adv. Mater.* **2013**, *25*, 5997; b) Z. L. Wang, *ACS Nano* **2013**, *7*, 9533.
[2] D. H. Kim, N. Lu, R. Ma, Y. S. Kim, R. H. Kim, S. Wang, J. Wu, S. M. Won, H. Tao, A. Islam, K. J. Yu, T. I. Kim, R. Chowdhury, M. Ying, L. Xu, M. Li, H. J. Chung, H. Keum, M. McCormick, P. Liu, Y. W. Zhang, F. G. Omenetto, Y. Huang, T. Coleman, J. A. Rogers, *Science* **2011**, *333*, 838.
[3] M. Kaltenbrunner, T. Sekitani, J. Reeder, T. Yokota, K. Kuribara, T. Tokuhara, M. Drack, R. Schwodiauer, I. Graz, S. Bauer-Gogonea, S. Bauer, T. Someya, *Nature* **2013**, *499*, 458.
[4] S. Gong, W. Schwalb, Y. Wang, Y. Chen, Y. Tang, J. Si, B. Shirinzadeh, W. Cheng, *Nat. Commun.* **2014**, *5*, 3132.
[5] A. N. Sokolov, B. C. Tee, C. J. Bettinger, J. B. Tok, Z. Bao, *Acc. Chem. Res.* **2012**, *45*, 361.
[6] D. Son, J. Lee, S. Qiao, R. Ghaffari, J. Kim, J. E. Lee, C. Song, S. J. Kim, D. J. Lee, S. W. Jun, S. Yang, M. Park, J. Shin, K. Do, M. Lee, K. Kang, C. S. Hwang, N. Lu, T. Hyeon, D. H. Kim, *Nat. Nanotechnol.* **2014**, *9*, 397.
[7] S. C. Mannsfeld, B. C. Tee, R. M. Stoltenberg, C. V. Chen, S. Barman, B. V. Muir, A. N. Sokolov, C. Reese, Z. Bao, *Nat. Mater.* **2010**, *9*, 859.
[8] K. Takei, T. Takahashi, J. C. Ho, H. Ko, A. G. Gillies, P. W. Leu, R. S. Fearing, A. Javey, *Nat. Mater.* **2010**, *9*, 821.
[9] D. J. Cohen, D. Mitra, K. Peterson, M. M. Maharbiz, *Nano. Lett.* **2012**, *12*, 1821.
[10] N. T. Tien, S. Jeon, D. I. Kim, T. Q. Trung, M. Jang, B. U. Hwang, K. E. Byun, J. Bae, E. Lee, J. B. Tok, Z. Bao, N. E. Lee, J. J. Park, *Adv. Mater.* **2014**, *26*, 796.
[11] V. Maheshwari, R. F. Saraf, *Science* **2006**, *312*, 1501.
[12] D.-W. Lee, Y.-S. Choi, *Microelectron. Eng.* **2008**, *85*, 1054.
[13] X. Liu, Y. Zhu, M. W. Nomani, X. Wen, T.-Y. Hsia, G. Koley, *J. Micromech. Microeng.* **2013**, *23*, 025022.
[14] S. Jung, J. H. Kim, J. Kim, S. Choi, J. Lee, I. Park, T. Hyeon, D. H. Kim, *Adv. Mater.* **2014**, *26*, 4825.
[15] S. Wagner, S. Bauer, *MRS. Bull.* **2012**, *37*, 207.
[16] T. Sekitani, Y. Noguchi, K. Hata, T. Fukushima, T. Aida, T. Someya, *Science* **2008**, *321*, 1468.
[17] a) T. Yamada, Y. Hayamizu, Y. Yamamoto, Y. Yomogida, A. Izadi-Najafabadi, D. N. Futaba, K. Hata, *Nat. Nanotechnol.* **2011**, *6*, 296; b) M. Park, J. Im, M. Shin, Y. Min, J. Park, H. Cho, S. Park, M. B. Shim, S. Jeon, D. Y. Chung, J. Bae, U. Jeong, K. Kim, *Nat. Nanotechnol.* **2012**, *7*, 803; c) B. Zhu, Z. Niu, H. Wang, W. R. Leow, H. Wang, Y. Li, L. Zheng, J. Wei, F. Huo, X. D. Chen, *Small* **2014**, *10*, 3625.
[18] a) H. B. Yao, J. Ge, C. F. Wang, X. Wang, W. Hu, Z. J. Zheng, Y. Ni, S. H. Yu, *Adv. Mater.* **2013**, *25*, 6692; b) Y. Tang, S. Gong, Y. Chen, L. W. Yap, W. L. Cheng, *ACS Nano* **2014**, *8*, 5707.
[19] C. L. Choong, M. B. Shim, B. S. Lee, S. Jeon, D. S. Ko, T. H. Kang, J. Bae, S. H. Lee, K. E. Byun, J. Im, Y. J. Jeong, C. E. Park, J. J. Park, U. I. Chung, *Adv. Mater.* **2014**, *26*, 3451.
[20] F. R. Fan, L. Lin, G. Zhu, W. Wu, R. Zhang, Z. L. Wang, *Nano. Lett.* **2012**, *12*, 3109.
[21] C. Pang, G. Y. Lee, T. I. Kim, S. M. Kim, H. N. Kim, S. H. Ahn, K. Y. Suh, *Nat. Mater.* **2012**, *11*, 795.
[22] Q. Gao, H. Meguro, S. Okamoto, M. Kimura, *Langmuir* **2012**, *28*, 17593.
[23] L. Pan, A. Chortos, G. Yu, Y. Wang, S. Isaacson, R. Allen, Y. Shi, R. Dauskardt, Z. Bao, *Nat. Commun.* **2014**, *5*, 3002.
[24] K. Liu, X. Yao, L. Jiang, *Chem. Soc. Rev.* **2010**, *39*, 3240.
[25] M. A. Meyers, J. McKittrick, P. Y. Chen, *Science* **2013**, *339*, 773.
[26] T. Sun, L. Feng, X. Gao, L. Jiang, *Acc. Chem. Res.* **2005**, *38*, 644.
[27] K. M. Wisdom, J. A. Watson, X. Qu, F. Liu, G. S. Watson, C. H. Chen, *Proc. Natl. Acad. Sci. USA* **2013**, *110*, 7992.
[28] H. Lee, B. P. Lee, P. B. Messersmith, *Nature* **2007**, *448*, 338.
[29] P. R. Sanberg, *Behav. Biol.* **1976**, *17*, 435.
[30] M. C. McAlpine, H. Ahmad, D. Wang, J. R. Heath, *Nat. Mater.* **2007**, *6*, 379.
[31] N. J. Douville, Z. Y. Li, S. Takayama, M. D. Thouless, *Soft Matter* **2011**, *7*, 6493.
[32] T. Adrega, S. P. Lacour, *J. Micromech. Microeng.* **2010**, *20*, 055025.
[33] J. Park, Y. Lee, J. Hong, M. Ha, Y-D. Jung, H. Lim, S. Y. Kim, H. Ko, *ACS Nano* **2014**, *8*, 4689.
[34] W-G. Bae, H. N. Kim, D. Kim, S-H. Park, H. E. Jeong, K-Y. Suh, *Adv. Mater.* **2014**, *26*, 675.
[35] X. W. Wang, Y. Gu, Z. P. Xiong, Z. Cui, T. Zhang, *Adv. Mater.* **2014**, *26*, 1336.

Received: October 14, 2014
Revised: November 2, 2014
Published online:

DOI: 10.1002/smll.201403036